Electronic Supplementary Material (ESI) for Molecular Systems Design & Engineering.

Engineering Plastic Phase Transitions via Solid Solutions: The Case of "Reordering Frustration" in Ionic Plastic Crystals of Hydroxyquinuclidinium Salts

Samet Ocak,[a] Rebecca Birolo,[b] Gianlucia Carì,[a] Simone Bordignon,[b] Michele R. Chierotti,*[b] Dario Braga,[a] Roberto Gobetto,[b] Tommaso Salzillo,*[c,d] Elisabetta Venuti,[c] Omer Yaffe,[d] and Simone d'Agostino*[a]

[a] Department of Chemistry „Giacomo Ciamician" The University of Bologna, Via F. Selmi, 2, 40126 Bologna, Italy.

[b] Department of Chemistry and NIS Centre The University of TurinVia P. Giuria 7, 10125 Torino, Italy.

[c] Department of Industrial Chemistry "Toso Montanari" The University of Bologna, Viale del Risorgimento 4, 40124, Bologna,Italy.

[d] Department of Chemical and Biological Physics Weizmann Institute of Science, Rehovot 76100, Israel.

Table of contents	Page

Table S1. Amounts of reagents used in the synthesis of the salts $[QH]_2SO_4 \cdot H_2O$ and [QH]X (X^- =BPh_4^-, PF_6^-, and BF_4^-).

	Ag_2SO_4 (mg / mmol)	$NaBPh_4$ (mg / mmol)	$AgPF_6$ (mg / mmol)	$AgBF_4$ (mg / mmol)
$[QH]_2SO_4 \cdot H_2O$	120 / 0.12	-	-	-
$[QH]BPh_4$	-	200 / 0.06	-	-
$[QH]PF_6$	-	-	150 / 0.06	-
$[QH]BF_4$	-	-	-	100 / 0.06
$[QH](PF_6)_{0.9}(BF_4)_{0.1}$	-	-	138 / 0.5	10.6 / 0.1
$[QH](PF_6)_{0.8}(BF_4)_{0.2}$	-	-	122 / 0.48	22 / 0.12
$[QH](PF_6)_{0.7}(BF_4)_{0.3}$	-	-	106 /0.42	34 / 0.18

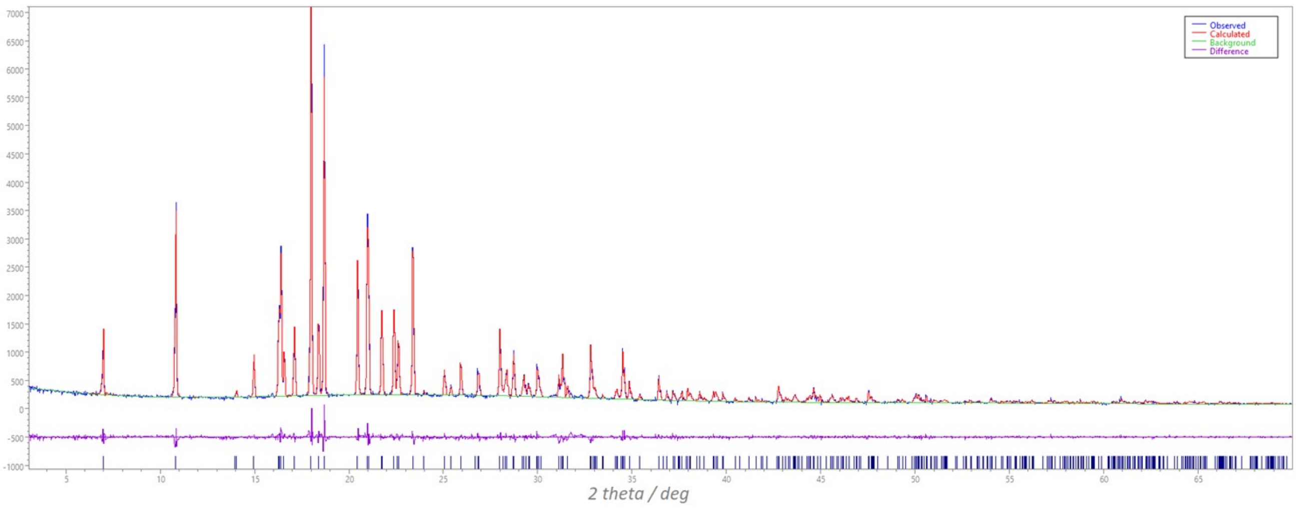

Fig. S1 Experimental (blue), calculated (red) powder XRD pattern of $[QH]_2SO_4 \cdot H_2O$ by Rietveld refinement and difference profile (magenta).

Table S2. Crystal data and refinement details for crystalline $[QH]_2SO_4{\cdot}H_2O$, $[QH]BPh_4$, $[QH]PF_6$, and $[QH]BF_4$. RT = room temperature phase, HT = high temperature phase, and LT = low temperature phase.

	$[QH]_2SO_4{\cdot}H_2O$ (powder data)	**$[QH]BPh_4$ (RT)**	**$[QH]BPh_4$ (LT)**	**[QH]PF6 (RT)**	**$[QH]PF_6$ (HT)***	**$[QH]BF_4$ (LT)**
Formula	$C_{14}H_{30}N_2O_7S$	$C_{31}H_{34}BNO$	$C_{31}H_{34}BNO$	$C_7H_{14}F_6NOP$	$C_7H_{14}F_6NOP$	$C_7H_{14}F_4NOB$
FW (g/mol)	370.464	447.40	447.40	273.16	273.16	215
Temperature/K	300	300	100	300	320	200
Crystal system	Monoclinic	Orthorhombic	Orthorhombic	Tetragonal	Cubic	Orthorhombic
Space group	$P2_1$	$P2_12_12_1$	$P2_12_12_1$	$P4_12_12$	P432	$P2_12_12_1$
a/Å	12.7496(3)	10.0708(5)	10.2152(4)	8.8859(4)	6.5126(7)	8.0330(8)
b/Å	10.7046(3)	13.3124(7)	12.9850(5)	8.8859(4)	6.5126(7)	9.7577(15)
c/Å	6.3468(2)	18.4685(9)	18.0958(10)	53.846(5)	6.5126(7)	12.6772(15)
α/°	90	90	90	90	90	90
β/°	96.550(1)	90	90	90	90	90
γ/°	90	90	90	90	90	90
Volume/Å^3	860.56(4)	2476.0(2)	2400.31(9)	4251.6(5)	276.23(9)	993.7(2)
Z	2	4	4	16	1	4
ρ_{calc} g/cm^3	1.430	1.200	1.238	1.707	1.642	1.437
μ/mm^{-1}	2.024	0.071	0.073	0.324	0.311	0.142
λ / Å	1.54056	0.71073	0.71073	0.71073	0.71073	0.71073
measd rflns	404	6434	7729	10456	873	2011
indep rflns	-	4083	5031	4917	90	1408
R_1	-	0.541	0.0861	0.0775	0.2704	0.0662
wR_2	-	0.1346	0.2161	0.1757	0.5555	0.1846

* = This crystal structure is not present in the CCDC; in case of need, ask the corresponding author SD.

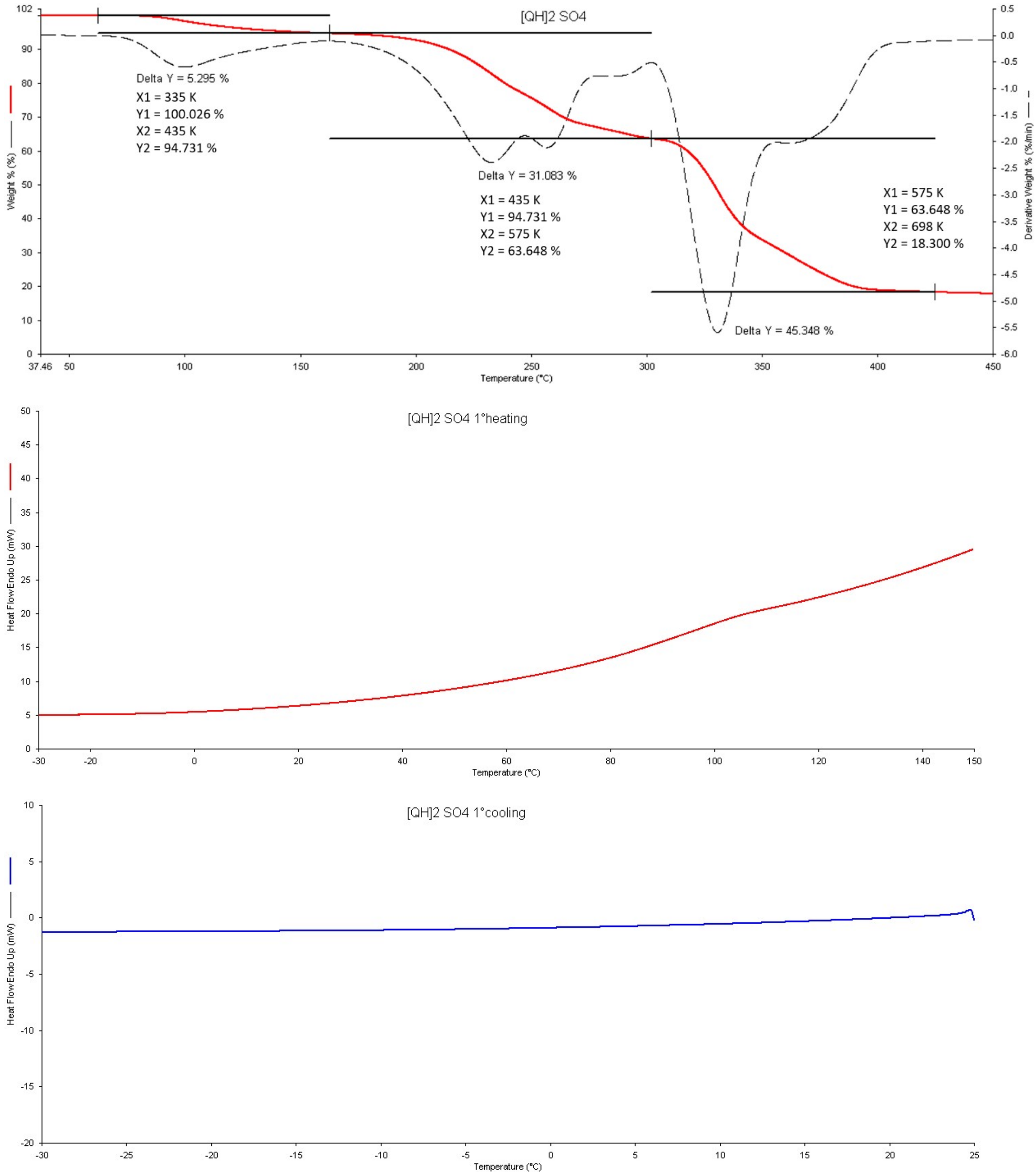

Fig. S2 TGA thermogram and DSC trace, heating cycle (red-line) and cooling cycle (blue-line), of $[QH]_2SO_4 \cdot H_2O$.

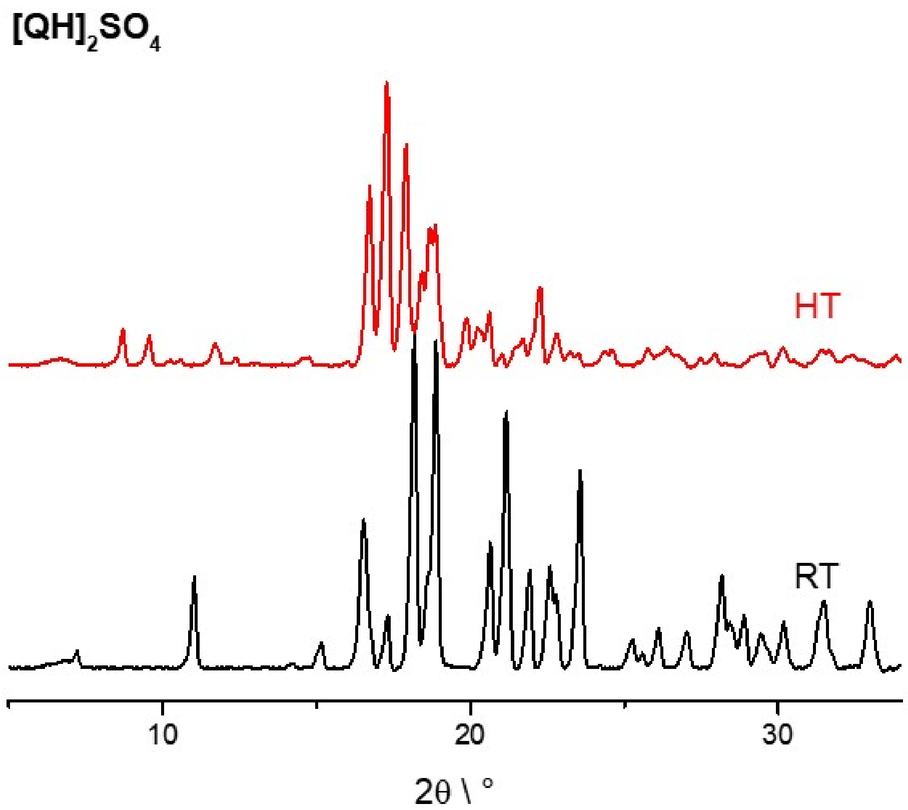

Fig. S3 Variable-temperature XRD patterns for $[QH]_2SO_4 \cdot H_2O$ recorded at RT and for its corresponding anhydrous phase $[QH]_2SO_4$ recorded at HT (413 K).

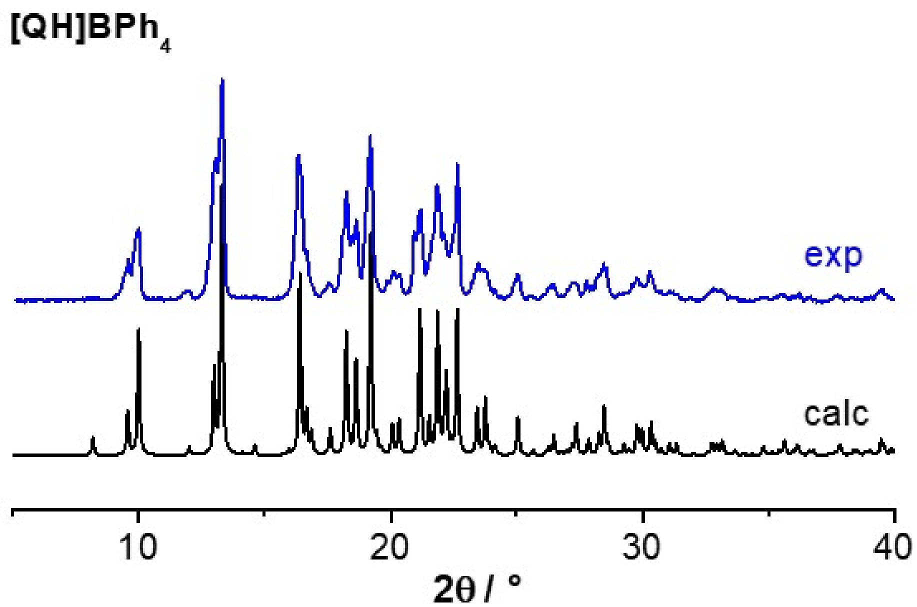

Fig. S4 Comparison between calculated (black) and experimental (blue) diffraction patterns for compound $[QH]BPh_4$ at LT.

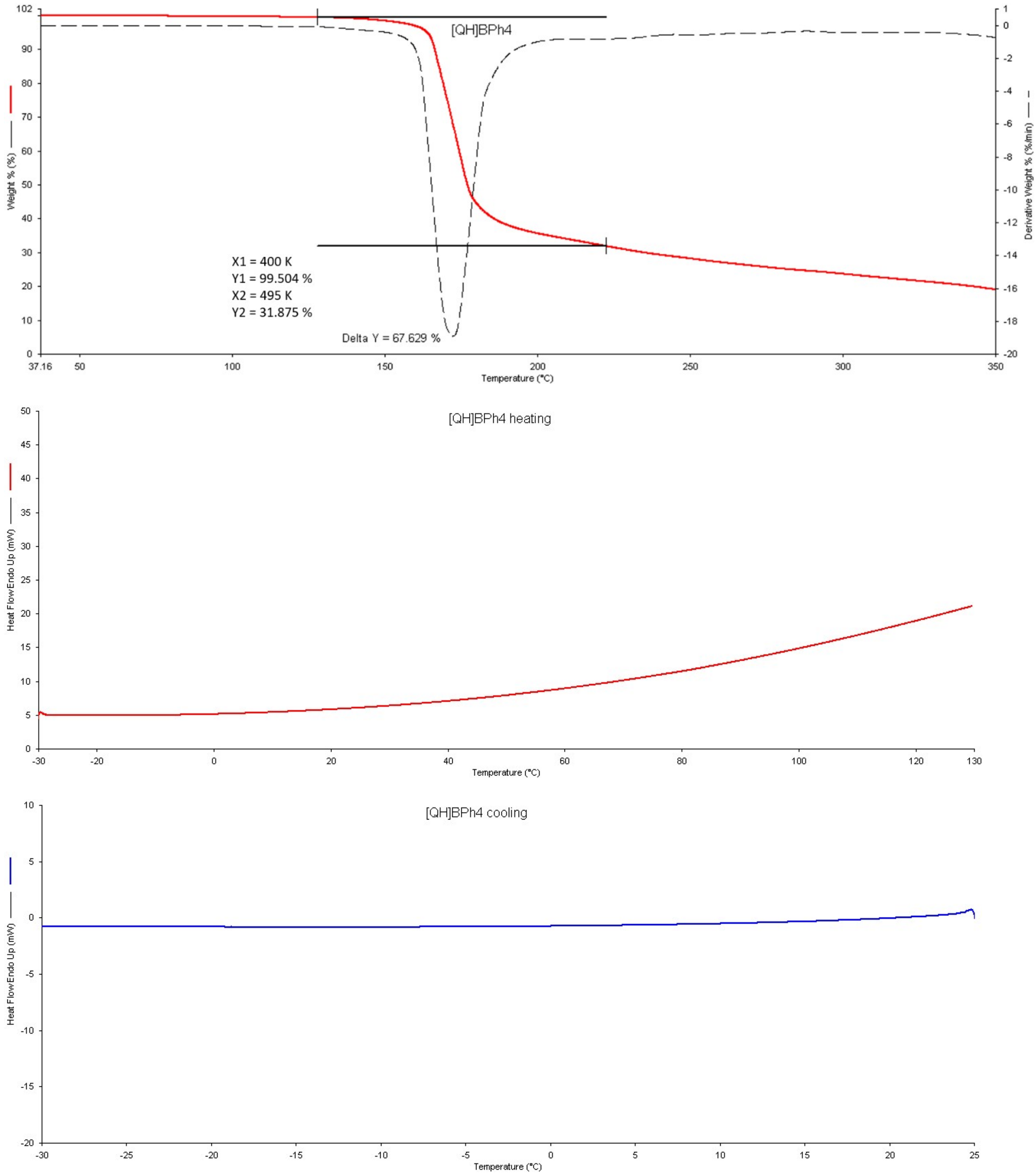

Fig. S5 DSC trace, heating cycle (red-line) and cooling cycle (blue-line), and TGA thermogram of [QH]BPh_4

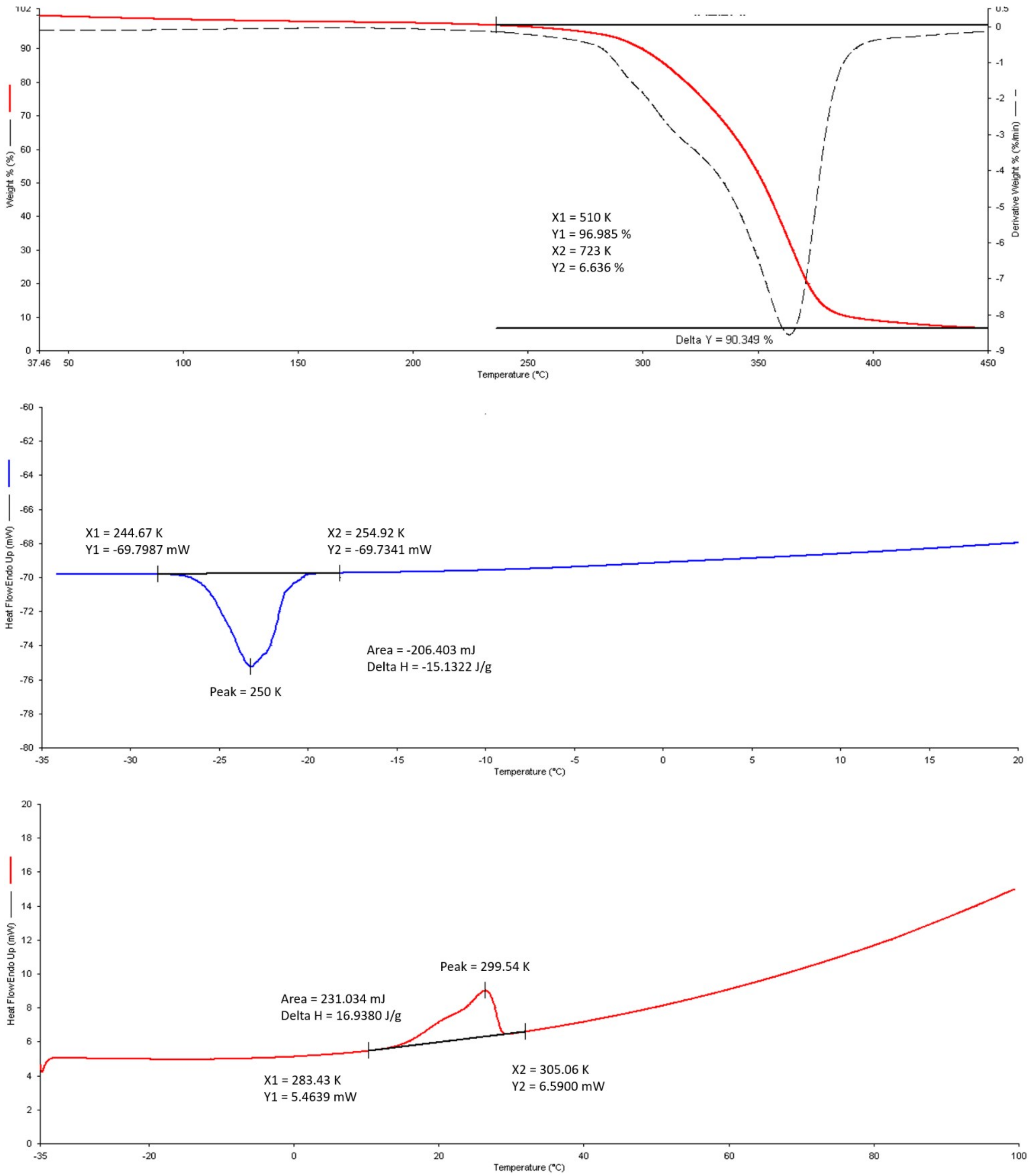

Fig. S6 DSC trace, heating cycle (red-line) and cooling cycle (blue-line), and TGA thermogram of $[QH]BF_4$.

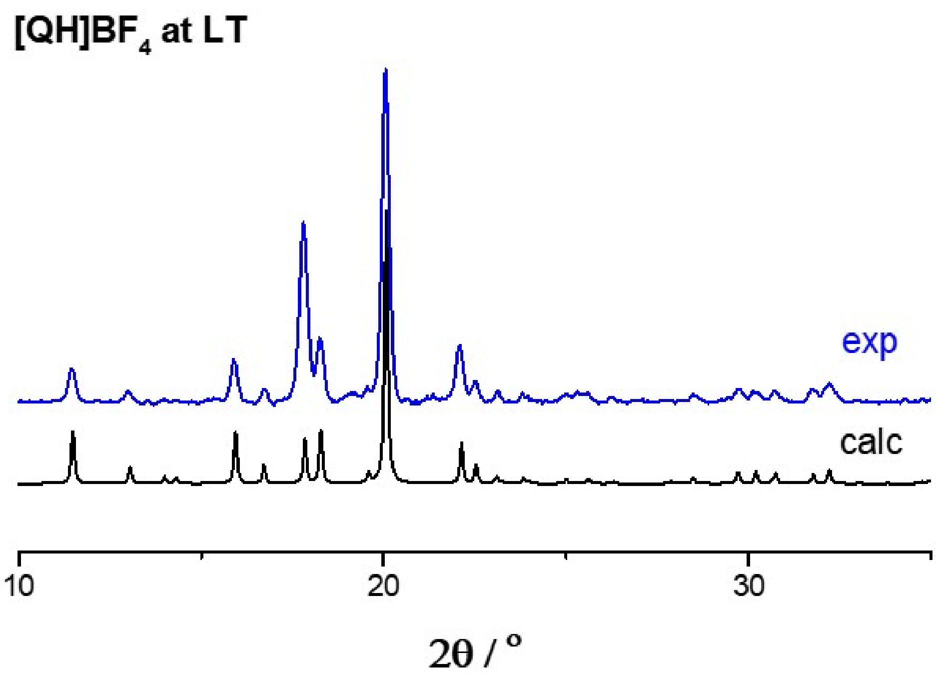

Fig. S7 Comparison between calculated (black) and experimental (blue) diffraction patterns for $[QH]BF_4$ at LT (200 K).

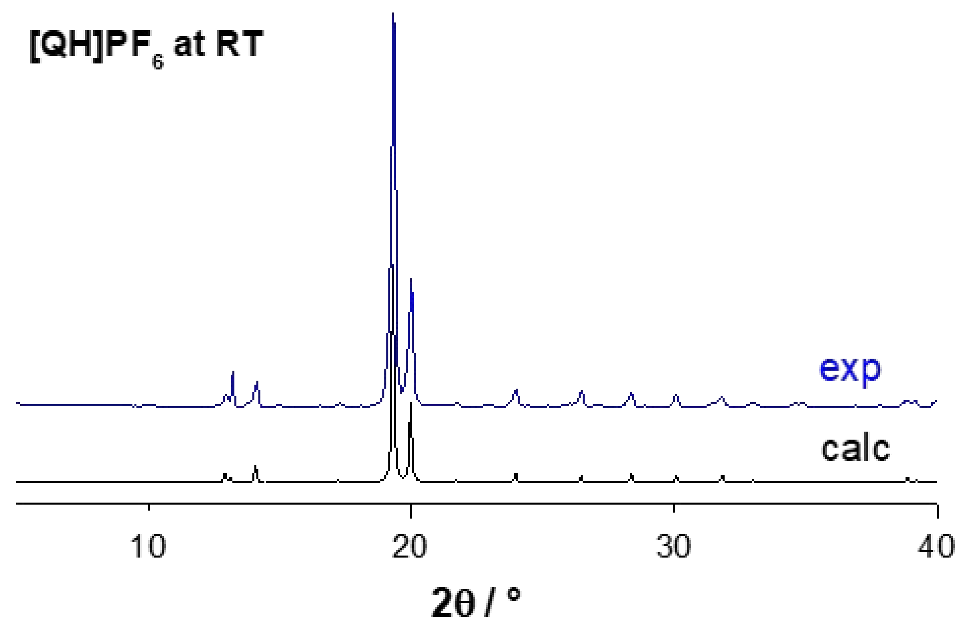

Fig. S8 Comparison between calculated (black) and experimental (blue) diffraction patterns for $[QH]PF_6$ at RT.

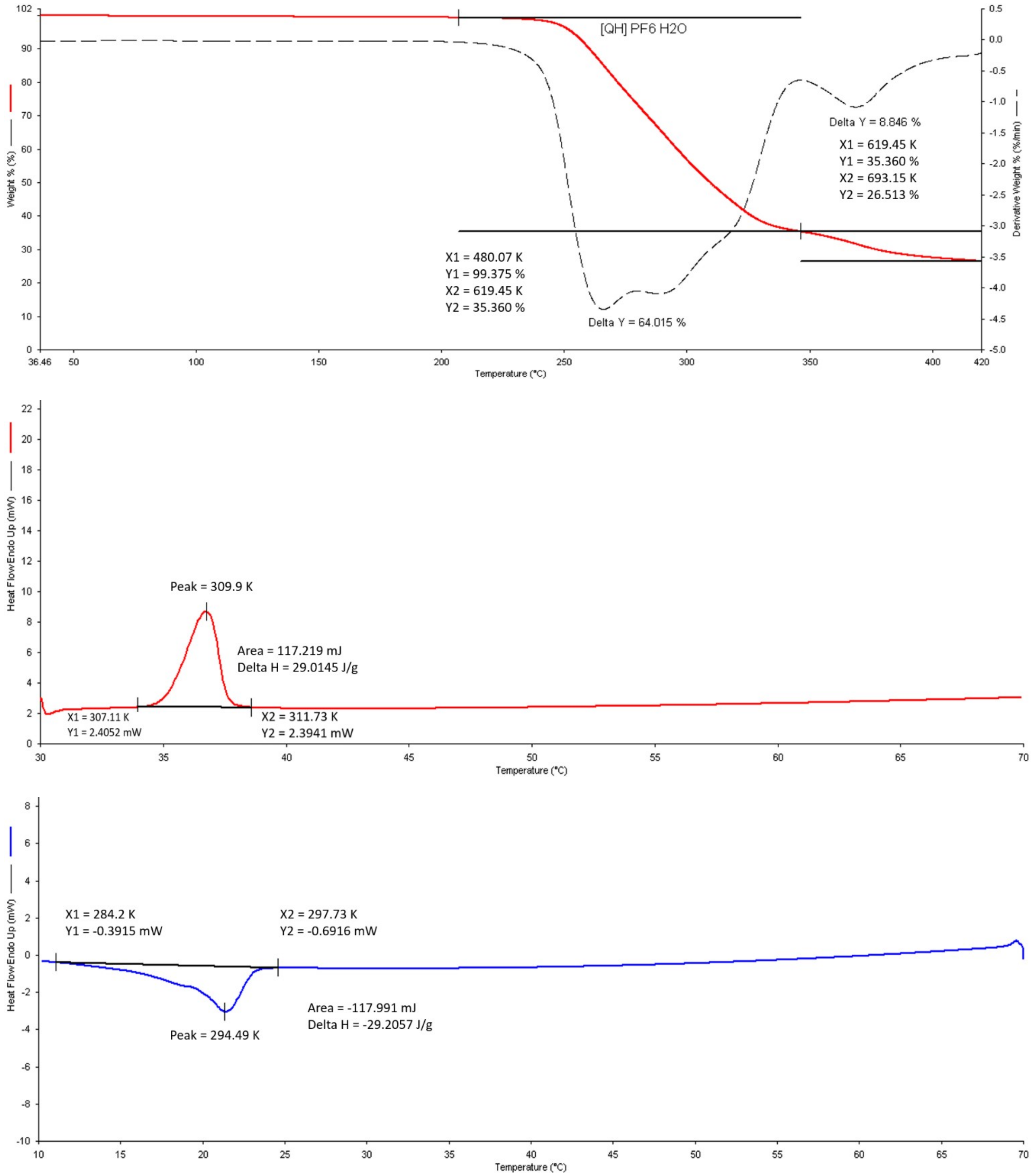

Fig. S9 DSC trace, heating cycle (red-line) and cooling cycle (blue-line), and TGA thermogram of [QH]PF_6.

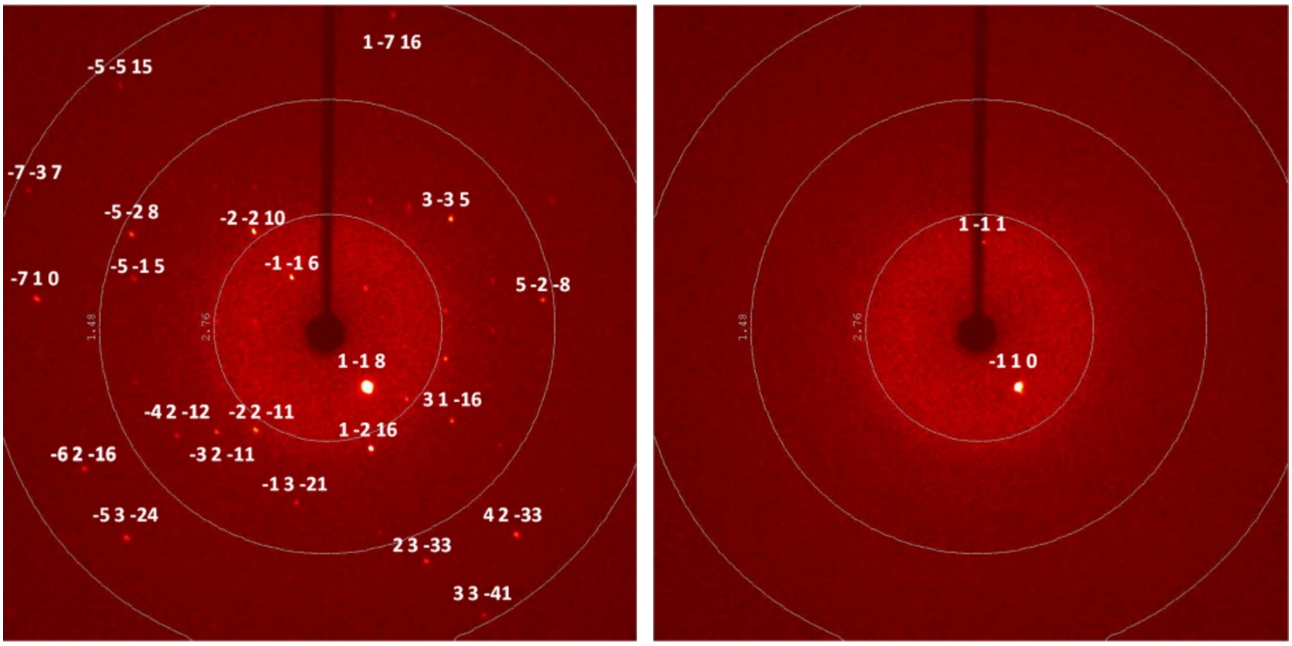

Fig. S10 φ-Scan images taken on a single crystal of $[QH]PF_6$ before (left) and after (right) the tetragonal-to-cubic phase transition.

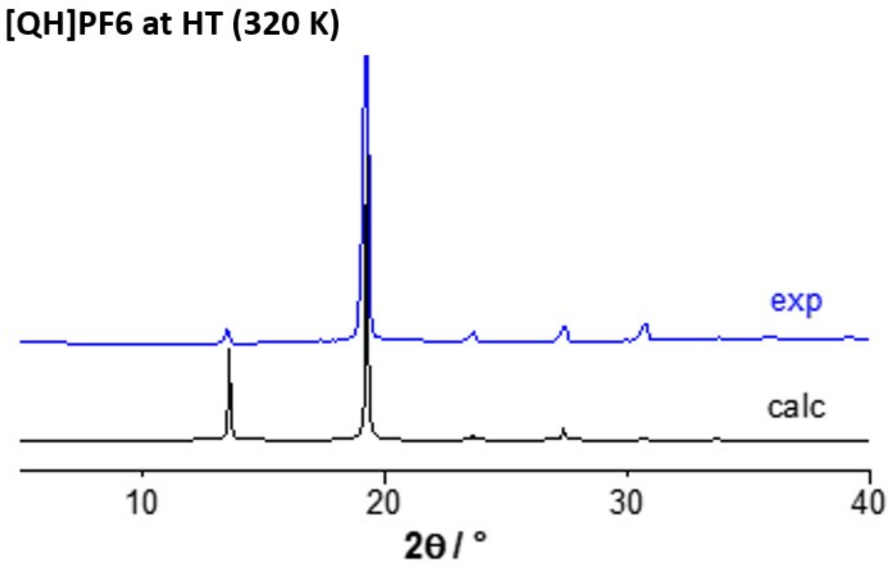

Fig. S11 Comparison between calculated (black) and experimental (red) diffraction patterns for $[QH]PF_6$ at HT (320 K).

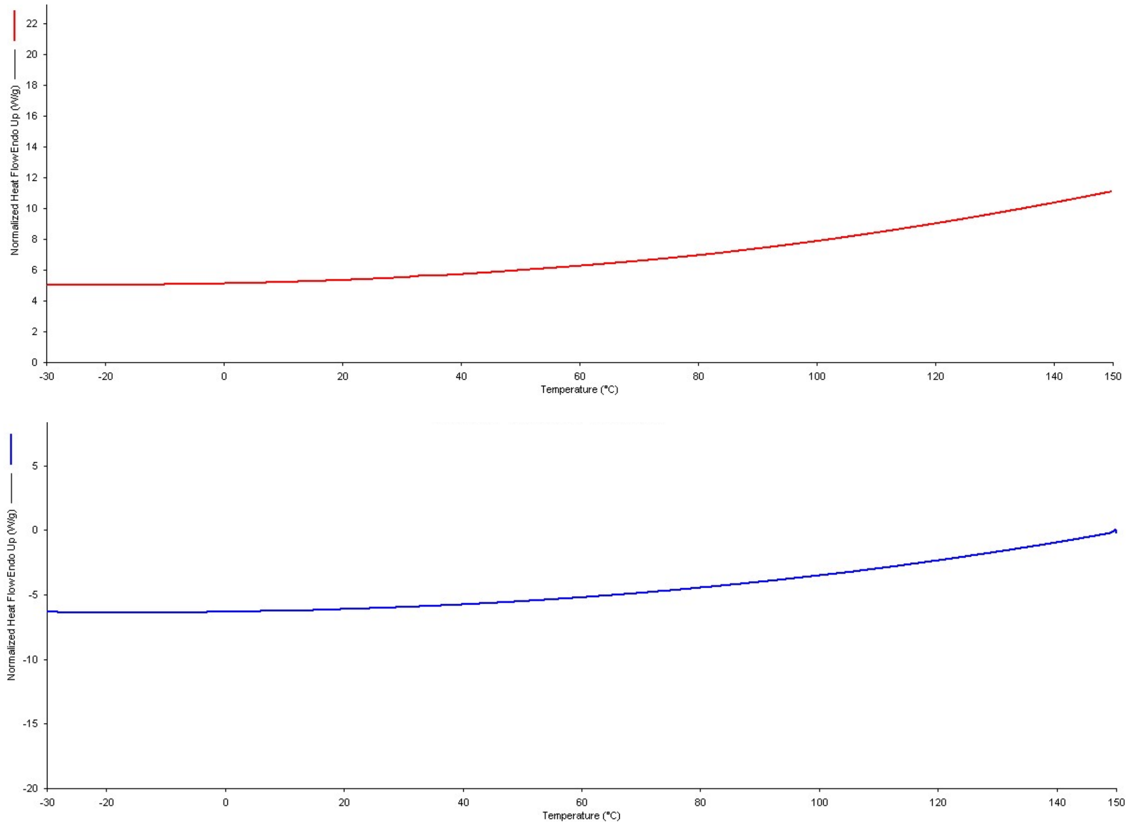

Fig. S12 DSC trace, heating cycle (red-line) and cooling cycle (blue-line) of $[QH](PF_6)_{0.9}(BF_4)_{0.1}$

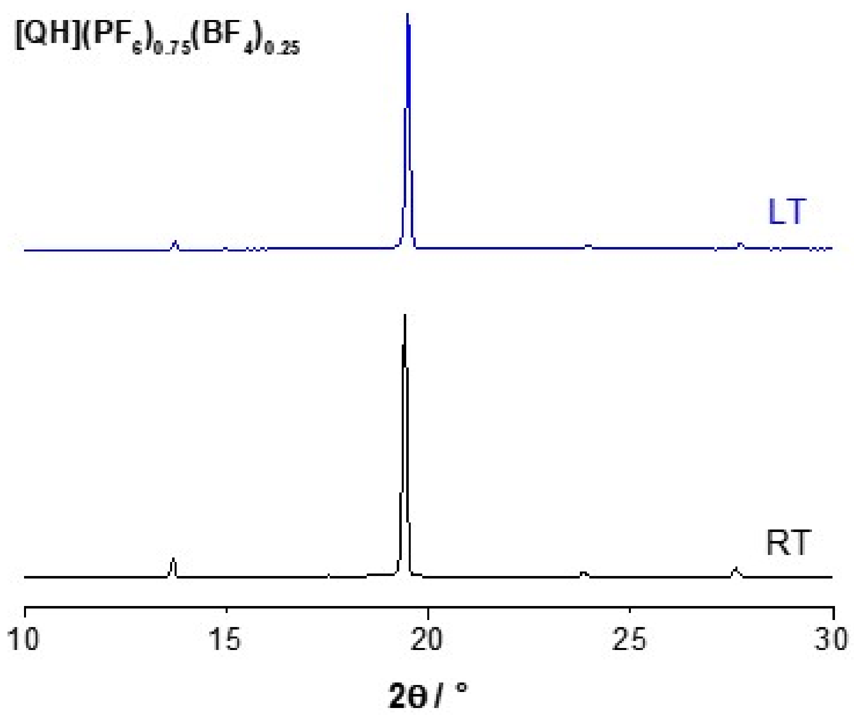

Fig. S13 Powder XRD patterns recorded at RT and at LT (123 K) for the solid solution $[QH](PF_6)_{0.7}(BF_4)_{0.3}$.

Table S3. ^{13}C SSNMR chemical shift values for $[QH]BF_4$, $[QH]PF_6$, $[QH](PF_6)_{0.9}(BF_4)_{0.1}$ and $[QH]BPh_4$.

	$[QH]BF_4$ (ppm)	**$[QH]PF_6$ (ppm)**	**$[QH](PF_6)_{0.9}(BF_4)_{0.1}$ (ppm)**	**$[QH]BPh_4$ (ppm)**
C(Ar)				165.5
CH(Ar)				136.0, 128.3, 127.5, 126.2, 123.5, 121.9
CH-OH	64.5	64.5	64.5	63.3
CH_2-N	56.6	56.7	56.7	56.7
CH_2-N	48.1	48.5	48.4	48.3
CH_2-N	47.1	47.5	47.4	46.0
CH	26.1	25.9	26.0	25.5
CH_2	20.5	20.4	20.4	18.9
CH_2	16.6	16.3	16.5	15.1

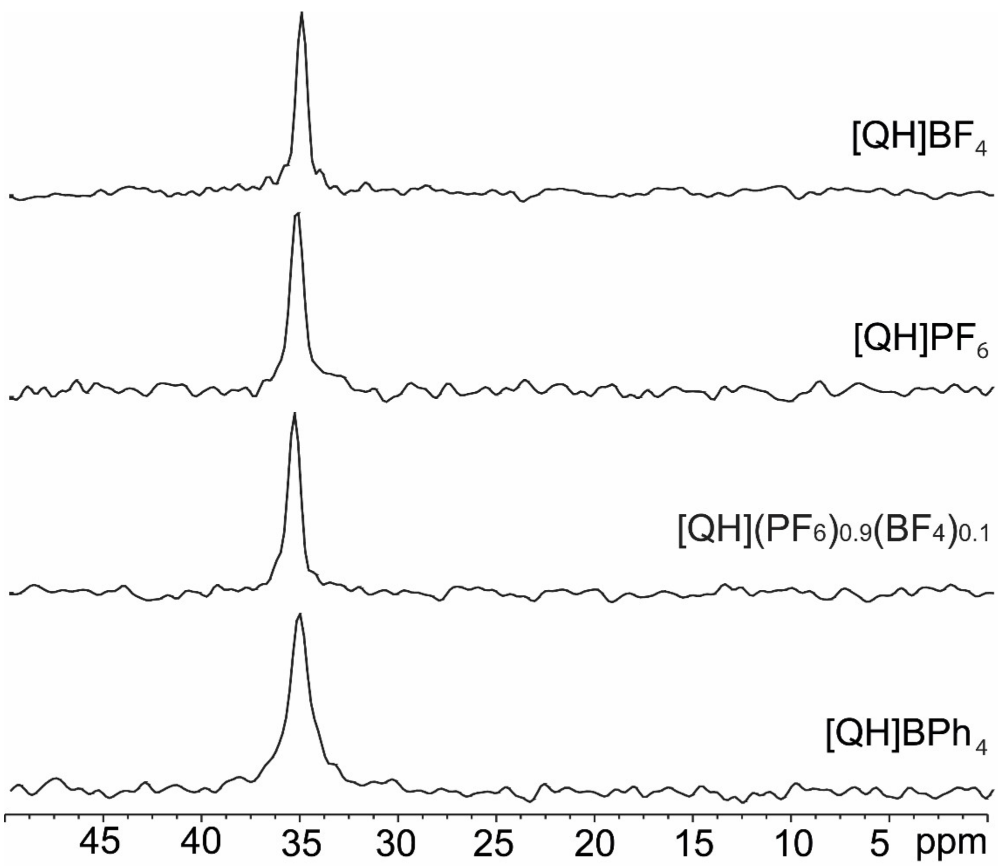

Fig. S14 ^{15}N (40.56 MHz) CPMAS spectra of $[QH]BF_4$, $[QH]PF_6$, $[QH](PF_6)_{0.9}(BF_4)_{0.1}$ and $[QH]BPh_4$, acquired at 12 kHz (room temperature).

Table S4. ^{15}N SSNMR chemical shift values for $[QH]BF_4$, $[QH]PF_6$, $[QH](PF_6)_{0.9}(BF_4)_{0.1}$ and $[QH]BPh_4$.

Salt	Chemical shift (ppm)
$[QH]BF_4$	35.2
$[QH]PF_6$	35.4
$[QH](PF_6)_{0.9}(BF_4)_{0.1}$	35.5
$[QH]BPh_4$	35.4

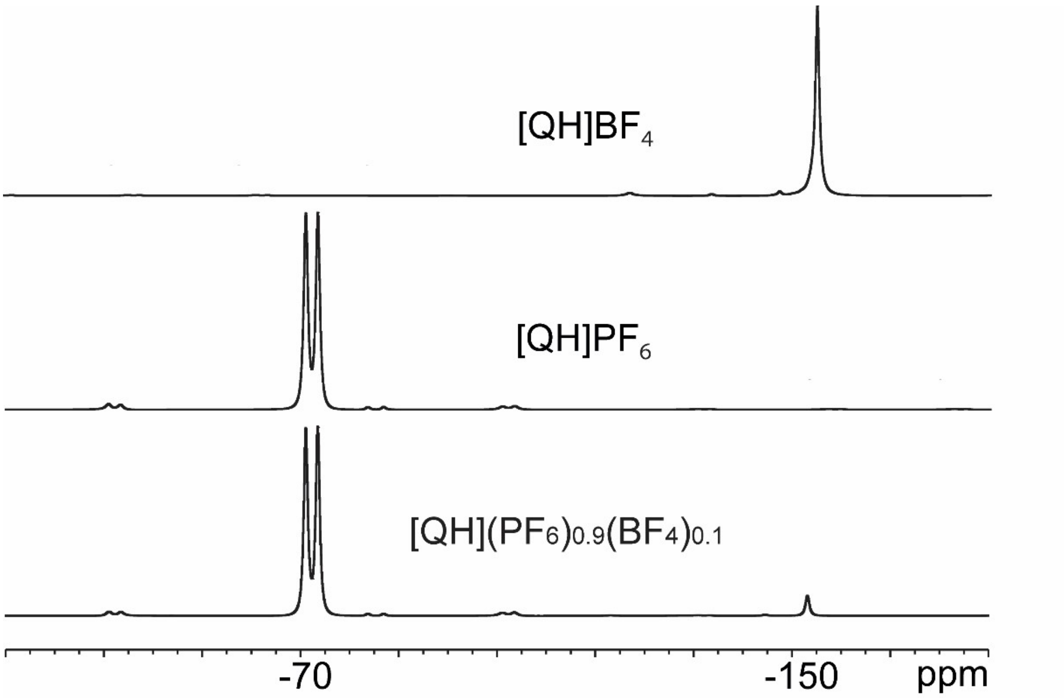

Fig. S15 ^{19}F (376.50 MHz) MAS spectra of $[QH]BF_4$, $[QH]PF_6$ and $[QH](PF_6)_{0.9}(BF_4)_{0.1}$, acquired at 12 kHz (room temperature).

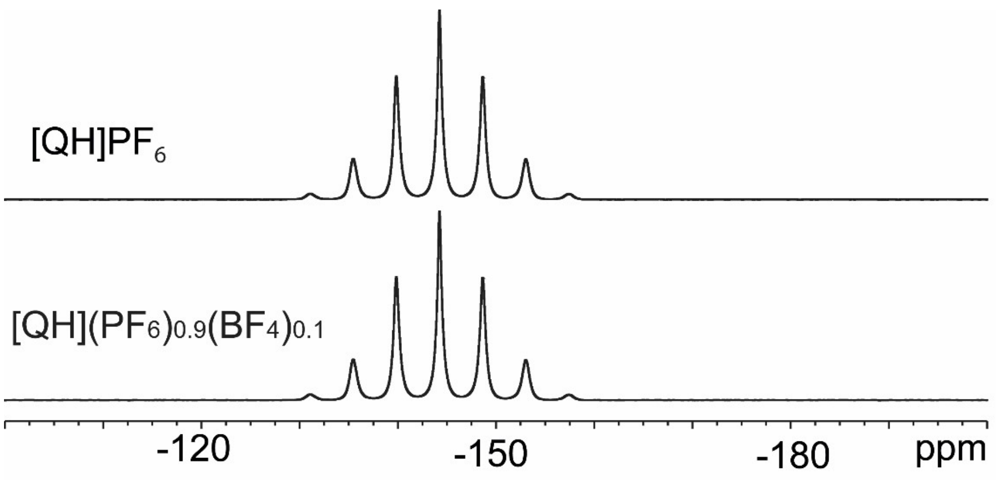

Fig. S16 ^{31}P (161.98 MHz) CPMAS spectra of $[QH]PF_6$ and $[QH](PF_6)_{0.9}(BF_4)_{0.1}$, acquired at 12 kHz (room temperature).

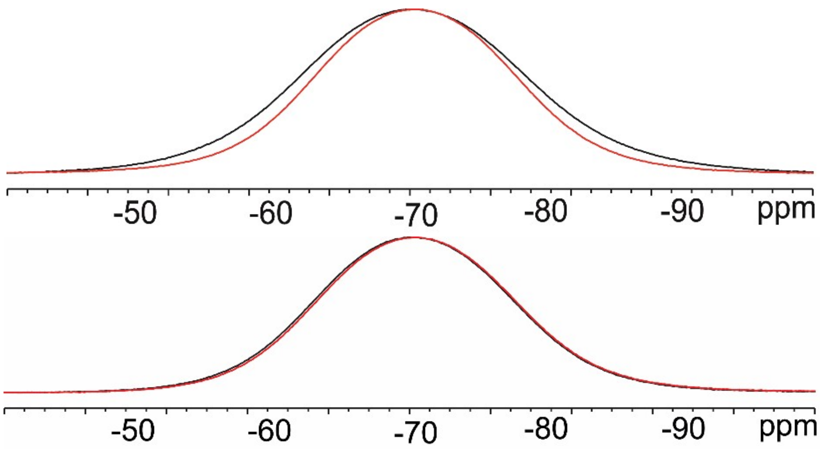

Fig. S17 ^{19}F (564.69 MHz) static spectra of $[QH]PF_6$ (top) and $[QH](PF_6)_{0.9}(BF_4)_{0.1}$ (bottom) at 298 K (black line) and 323 K (red line).

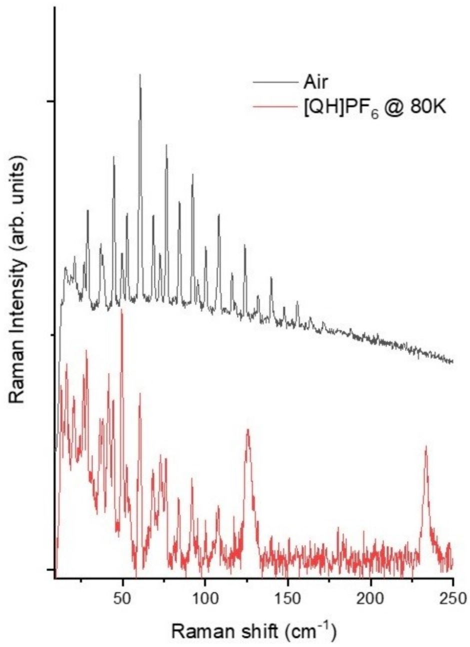

Fig. S18 Comparison of the air and of the ordered phase of $[QH]PF_6$ spectra in the low-frequency range.